

Applicability of variability response function for geotechnical risk assessment

M. K. Lo

Ph.D. Student, Dept. of Civil and Environmental Engineering, The Hong Kong Polytechnic University, Hong Kong

Y. F. Leung

Assistant Professor, Dept. of Civil and Environmental Engineering, The Hong Kong Polytechnic University, Hong Kong

ABSTRACT: This paper explores the use of variability response function (VRF) for risk assessment of geotechnical system under spatially variable soil properties, where the properties exhibit a range of possible autocorrelation characteristics. VRF only requires a single set of analysis, but traditional Monte Carlo simulation (MCS) requires separate sets of analyses. VRF can be estimated through a simple regression procedure, which does not require random field simulation. In a footing displacement analysis, the reliability assessments by VRF match well with those of MCS, when the soil property has relatively low variance.

For a geotechnical system with spatially variable soil properties, the response uncertainty depends heavily on the spatial autocorrelation distances. For example, the uncertainty in footing displacement increases monotonically with the vertical autocorrelation distance of Young's modulus (Al-Bittar and Soubra 2014). According to a recent study of pile group reliability by Leung and Lo (2018), there exists a horizontal autocorrelation distance of soil modulus that corresponds to the largest uncertainty in differential settlements across the foundation.

However, due to limited geotechnical investigation data, accurate determination of autocorrelation distances of soil properties is difficult. The values suggested in literature (e.g., Phoon and Kulhawy 1999) entail a wide range. Even if there are soil samples obtained at the site, the values derived from the samples will involve substantial statistical uncertainty, as noted in Ching et al. (2016). Therefore, a comprehensive reliability assessment of geotechnical structure should involve a range of possible values of autocorrelation distances. The traditional Monte Carlo Simulation (MCS) approach is able to

accomplish this task, but the associated computational effort is unpractically high, because a separate set of simulation is required for each autocorrelation distance. A certain set of simulation cannot be reused to analyze the reliability under another autocorrelation distance. Therefore, in this paper, the possibility of using only a single set of simulation to assess the reliability under different autocorrelation distances will be explored.

A potential approach for this problem is to define a response function, which is independent of spatial autocorrelation, in order to transfer the random soil profile into the random model response. For statically determinate structures, the transfer function can be analytically derived. In the study of Shinozuka (1987), a bar is subjected to an axial force, with the flexibility (inverse of Young's modulus) of the bar modelled as a random field. The derived response function for the bar displacement only depends on the mean flexibility, the bar geometry and the axial force, and does not depend on the spatial variation of flexibility. For statically indeterminate structures, the existence

of response function has not been proven, but it is possible to assume that it does, and then numerically test the effectiveness of the approach. Papadopoulos and Kokkinos (2012) and Manitaras et al. (2017) applied the response function approach to analyze statically indeterminate structures such as structural frames and 2-dimensional elastic soils, with the flexibility modelled as random fields. The reliability computed from response function matched with that from MCS, when the coefficient of variation for flexibility is sufficiently small.

While previous studies on response functions mainly focused on building structures, this paper will examine the applicability of response functions on shallow footing displacements. It begins with the theory of response function, followed by a simulation scheme to determine the function. The framework will then be illustrated through analyses of footing displacements.

1. INTRODUCTION TO VARIABILITY RESPONSE FUNCTION

A variance response function (VRF) can be defined to transform the spectral density of soil profiles into the variance of the response g . For a 1-dimensional soil profile varying in x -direction:

$$\text{Var}(g) = \int_{-\infty}^{\infty} \text{VRF}(\omega_x) S(\omega_x) d\omega_x \quad (1)$$

where ω_x is the spatial frequency in x -direction. $S(\omega_x)$ is spectral density, which is the Fourier transform of spatial autocovariance function $C(\Delta x)$, Δx being the spatial lag:

$$S(\omega_x) = \frac{1}{2\pi} \int_{-\infty}^{\infty} e^{-i\omega_x \Delta x} C(\Delta x) d\Delta x \quad (2)$$

Table 1 and Figure 1 show the spectral densities of two common autocorrelation functions.

Table 1: Two common autocorrelation functions and their spectral densities. σ^2 =random field variance; θ_x =autocorrelation distance.

	$C(\Delta x)$	$S(\omega_x)$
Single exponential	$\sigma^2 \exp\left(-\frac{\Delta x}{\theta_x}\right)$	$\frac{\sigma^2 \theta_x}{\pi(1 + \omega_x^2 \theta_x^2)}$
Squared exponential	$\sigma^2 \exp\left(-\frac{\Delta x^2}{\theta_x^2}\right)$	$\frac{\sigma^2 \theta_x}{2\sqrt{\pi}} \exp\left(-\frac{\omega_x^2 \theta_x^2}{4}\right)$

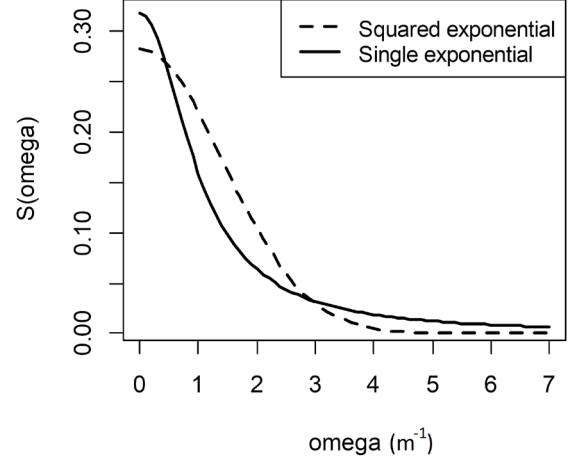


Figure 1: Spectral densities of two autocorrelation functions with $\sigma^2 = 1$ and $\theta_x = 1$.

According to Eq. (1), VRF indicates the amount of response variance contributed by each sinusoid that comprises the random field. This concept can be made clearer by rewriting Eq. (1) in discrete form:

$$\text{Var}(g) = \lim_{n \rightarrow \infty} \sum_{n=-K}^K \text{VRF}(\omega_n) S(\omega_n) \Delta\omega \quad (3)$$

In Eq.(3), $S(\omega_n) \Delta\omega$ is the variance of the n -th sinusoid that comprises the random field. The variance of the n -th sinusoid is transformed into the variance of the response, by multiplying with the VRF. The response variance contributed by each sinusoid can be added independently to yield the total response variance.

A mean response function (MRF) can be similarly defined to transform the spectral density of soil profile into the mean response:

$$E(g) = \int_{-\infty}^{\infty} \text{MRF}(\omega)S(\omega)d\omega \quad (4)$$

Finally, the definition of VRF or MRF can be extended to 2-dimensional or 3-dimensional problems. For a 2-dimensional VRF:

$$\text{Var}(g) = \int_{-\infty}^{\infty} \int_{-\infty}^{\infty} \text{VRF}(\omega_x, \omega_y)S(\omega_x, \omega_y)d\omega_x d\omega_y \quad (5)$$

2. SIMULATION SCHEME TO ESTIMATE VRF AND MRF

The analytical form of VRF can only be derived for simple structures. For practical applications to geotechnical problems, VRF can be estimated by simulation instead. The scheme proposed in this section is extended from the works of Papadopoulos and Kokkinos (2012) and Manitaras et al. (2017). Extra elements include modeling of the system response by cosine equation, and estimating VRF from the mean and amplitude of the cosine equation. The extended scheme is shown later to be more accurate, when estimating VRF in the low frequency region.

The proposed steps for the simulation scheme would be:

1. Set a positive frequency range $[0, \omega_u]$ for VRF determination. The cut-off frequency ω_u depends on the smallest autocorrelation distance θ_s (i.e. the autocorrelation distances to be analyzed range from θ_s to ∞). To preserve $\alpha\%$ of random field variance,

$$\int_0^{\omega_u} 2S(\omega)d\omega = \frac{\alpha}{100} \sigma^2 \quad (6)$$

where $S(\omega)$ is the spectral density corresponding to θ_s .

2. Partition the range $[0, \omega_u]$ into $(M + 1)$ intervals. A simple method is to partition into equal intervals: $\omega_i = i\Delta\omega$, with $i = 0, 1, \dots, M$ and $\Delta\omega = \omega_u/M$.

3. For a particular frequency ω_i , simulate $N \approx 5$ to 10 soil profiles with cosine spatial variation:

$$z(x) = \mu + \sqrt{2}\sigma \cos(\omega_i x + \phi_n) \quad (7)$$

ϕ_n is the center of intervals $(\frac{2\pi n}{N}, \frac{2\pi(n+1)}{N})$ for $n = 0, 1, \dots, N - 1$.

4. For a particular frequency ω_i , the model response g due to different phases ϕ_n should be periodic around an average level of $\bar{g}(\omega_i)$. If g varies with ϕ_n in a cosine equation, the amplitude of the wave can be denoted as $A(\omega_i)$. $\bar{g}(\omega_i)$ and $A(\omega_i)$ can be empirically estimated by linear regression:

$$\begin{bmatrix} \hat{g}(\omega_i) \\ \beta_1 \\ \beta_2 \end{bmatrix} = (\mathbf{X}^T \mathbf{X})^{-1} \mathbf{X}^T \mathbf{g}$$

where $\mathbf{X} = \begin{bmatrix} 1 & \cos(\phi_1) & \sin(\phi_1) \\ \vdots & \vdots & \vdots \\ 1 & \cos(\phi_N) & \sin(\phi_N) \end{bmatrix}$ (8)

$$\mathbf{g} = \begin{bmatrix} g(\omega_i, \phi_1) \\ \vdots \\ g(\omega_i, \phi_N) \end{bmatrix}$$

$$\hat{A}(\omega_i) = \sqrt{\beta_1^2 + \beta_2^2}$$

5. The MRF and VRF at frequency ω_i are given by

$$\begin{aligned} \text{MRF}(\omega_i) &= \frac{\hat{g}(\omega_i)}{\sigma^2} \\ \text{VRF}(\omega_i) &= \frac{\hat{A}^2(\omega_i)}{2\sigma^2} \end{aligned} \quad (9)$$

6. Repeat Steps 3-6 for all frequencies ω_i , with $i = 0, 1, \dots, M$.
7. Use spline interpolation to interpolate VRF and MRF values at other frequencies.

Once the $\text{VRF}(\omega)$ and $\text{MRF}(\omega)$ are determined, $\text{Var}(g)$ and $E(g)$ under arbitrary spatial autocorrelation distance θ can be evaluated by integrating Eq. (1) and Eq. (4) numerically. To check whether the chosen frequency range $[0, \omega_u]$ is adequate in

representing the entire VRF or MRF curve, $VRF(\omega)$ should decay to zero at large ω , where the spatial variation is too rapid that its effect to the model response would be averaged out. Meanwhile, $\sigma^2 MRF(\omega)$ should decay to the deterministic model response. If such decay is not observed, more simulations should be done to find out the VRF or MRF at higher frequency ranges.

Using Eq. (4) alone to evaluate $E(g)$ will result in a slight underestimation, in the order of several percent, since $MRF(\omega)$ decays to a non-zero value. This can be avoided by adding an adjustment term, which is the truncated random field variance times the MRF asymptote (i.e. value of MRF as $\omega \rightarrow \infty$). The truncated random field variance is

$$\sigma^2 - \int_0^{\omega_u} 2S(\omega)d\omega \quad (10)$$

where $S(\omega)$ is the spectral density corresponding to θ , the autocorrelation distance under investigation.

3. FOOTING DISPLACEMENT ANALYSIS BY VRF AND MRF

The proposed simulation scheme is applied to analyze footing displacements, using the *FLAC* software. The *FLAC* model is 15 m wide, 6 m deep, with a rigid strip footing of width $B=2$ m located at the ground surface. The footing is subjected to a vertical load of 514 kPa, and the soil-footing interface is perfectly rough. The Young's modulus of the soil is modelled as a vertical normal random field with mean value 60 MPa and standard deviation of 9 MPa, corresponding to coefficient of variation (CV) of 0.15. The Poisson's ratio is a constant of 0.499. Figure 2 shows the footing geometry.

The smallest vertical autocorrelation length considered in the analyses is $\theta_s = 0.4 m = 0.2B$. With the squared exponential autocorrelation function, the cutoff frequency ω_u is $7m^{-1}$, in order to preserve 95% of random field variance. Since a high frequency spatial variation in Young's modulus leads to smaller

variation in footing displacement, when deciding the frequencies for VRF estimation, the lower frequency points are more closely spaced. In this study, $\omega = (0, 0.2, 0.4, 0.6, 0.8, 1, 1.25, 1.5, 1.75, 2, 2.5, 3, 3.5, 4, 4.5, 5, 6, 7) m^{-1}$, amounting to a total of $M = 18$ frequency points. For each frequency point, $N = 10$ Young's modulus profiles are simulated, with each profile being a cosine wave of different phase. Therefore, the total number of analyses is $18 \times 10 = 180$.

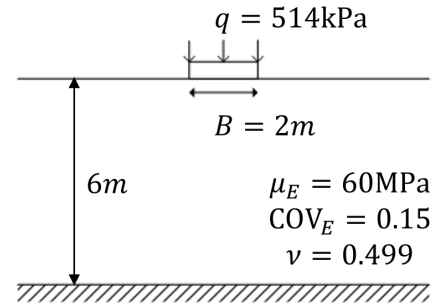


Figure 2: Footing geometry.

Figure 3 shows the footing displacement at different spatial frequencies ω and phases ϕ . When ω is zero (soil is homogeneous), the amplitude of displacement (i.e. $A(\omega)$) is the largest. When ω increases, $A(\omega)$ decreases. Figure 4 compares the displacement fitted by the cosine equation with the displacement computed by *FLAC*. The cosine equation can fit the displacement data satisfactorily, with goodness of fit $R^2 = 0.993$.

Figure 5 shows the VRF computed from $A(\omega)$ by Eq. (9). VRF can also be estimated empirically by directly calculating the variance using the displacements of the same spatial frequency. This empirical VRF is also plotted in Figure 5. From the figure, it appears that empirical estimation of VRF may lead to overestimation. To verify this proposition, another set of analysis is performed using $N=20$ phases, and the empirical VRF is also plotted. When the number of phase increases, the empirical VRF approaches the regression VRF. Therefore, the regression-based VRF should be the more robust estimate.

Figures 6 and 7 show the computed VRF and MRF points through linear regression, overlapped with the spline interpolated curves. According to the VRF curves, most of the variance of footing displacement is contributed by Young's modulus variation with frequency smaller than 2 m^{-1} , or a spatial period larger than $2\pi/\omega = 3.14 \text{ m} \approx 1.5B$. Meanwhile, the normalized MRF curve shows a decay from the peak value to the value of deterministic footing displacement (11.08 mm).

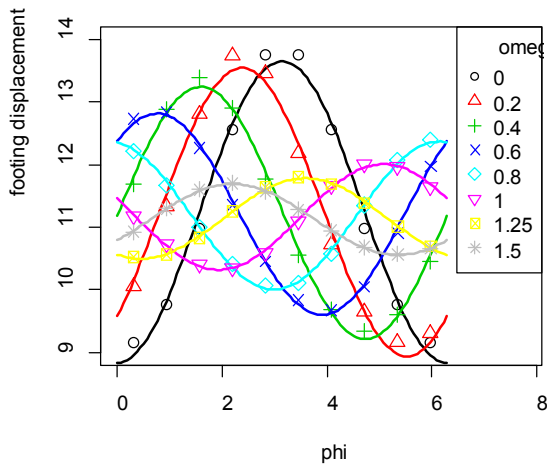


Figure 3: Footing displacement at different spatial frequencies and phases.

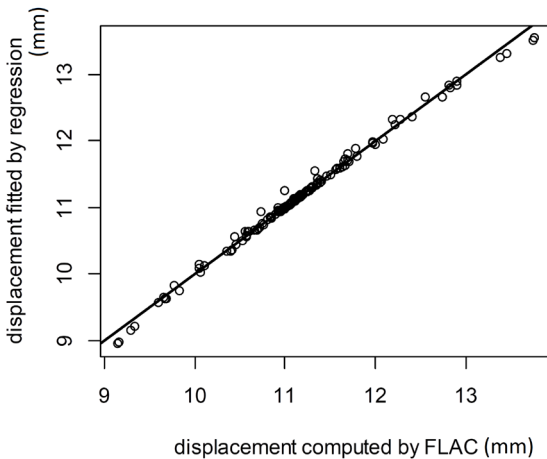


Figure 4: Comparison of fitted displacement and original displacement data by FLAC.

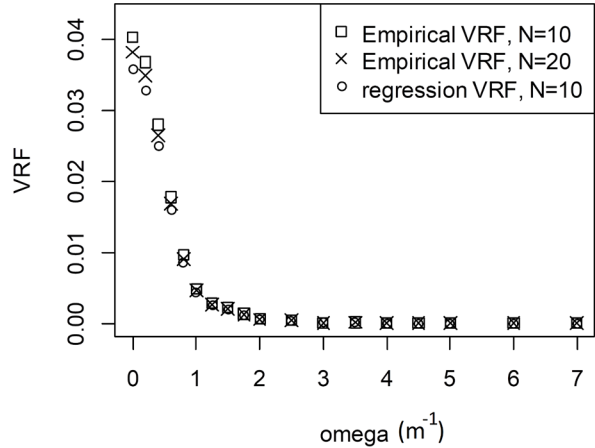


Figure 5: Comparing VRF estimated by regression and empirical approach

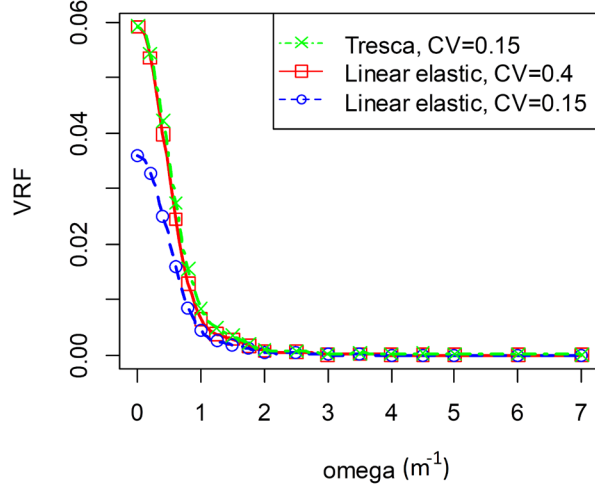


Figure 6: Computed VRF points overlapped with spline interpolated curves.

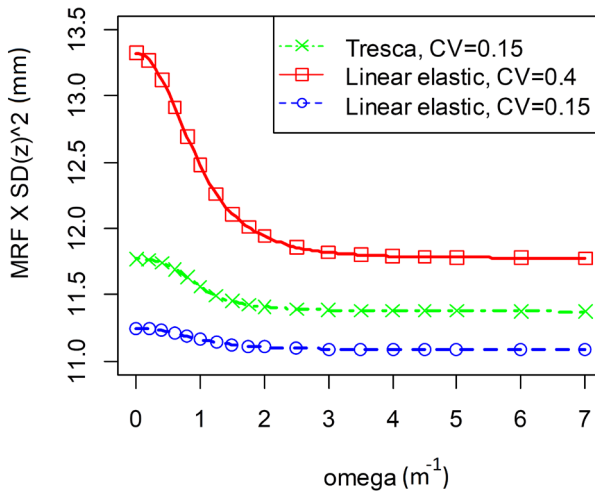


Figure 7: Normalized MRF points with spline interpolated curves.

To calculate the variance of footing displacement under a certain autocorrelation length of Young's modulus, the spectral density is multiplied with the VRF, and then numerically integrated. Figures 8 and 9 show the standard deviation and mean of footing displacements under various autocorrelation lengths, normalized by the footing width B . To validate the accuracies of the obtained statistics, Monte Carlo Simulations are conducted for three autocorrelation lengths ($B/\theta = 1, 2, 3$). Each MCS consists of 300 simulations. The MCS results are also plotted in Figures 8 and 9, which closely match with that obtained by VRF.

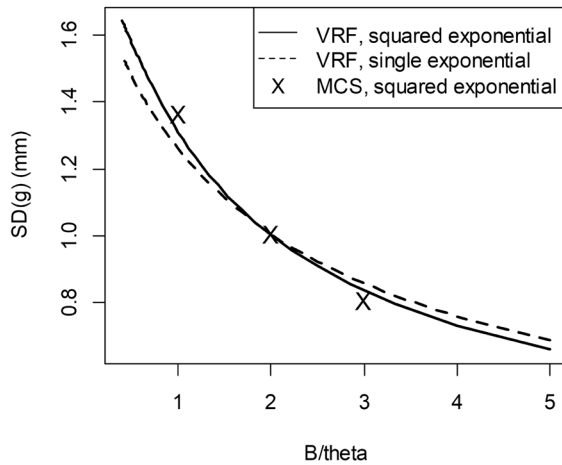


Figure 8: Standard deviation of footing displacement under different autocorrelation distances.

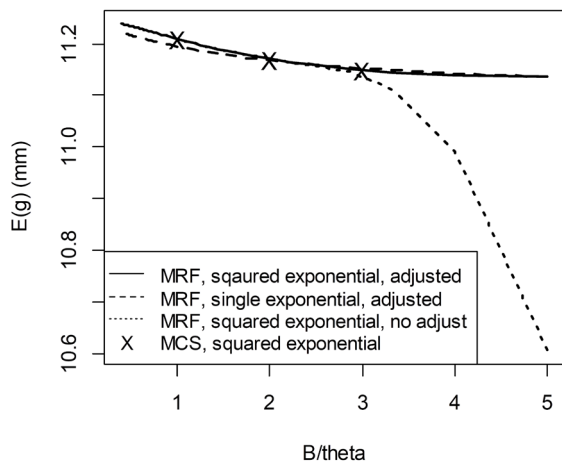


Figure 9: Mean of footing displacement under different autocorrelation distances.

The VRF approach slightly underestimates the response SD at large autocorrelation distance, and there is slight overestimation at low autocorrelation distance. Meanwhile, the mean responses obtained from both approaches match almost exactly, provided that the adjustment term is added when using the MRF approach. The validation also demonstrates significant saving in computational cost. Three separated sets of MCS, or a total of 900 analyses are required to compute 3 discrete points in Figure 8, whereas only a single set of 180 analyses can produce a continuous curve using VRF approach.

Next, the same set of 180 analyses is used again to examine the footing behavior under single exponential autocorrelation function. Although the cutoff frequency under single exponential function is significantly higher ($\omega_u = 32 \text{ m}^{-1}$ to preserve 95% of random field variance), no extra *FLAC* analyses are required, because from the VRF curve at Figure 6, the variance contributed by $\omega > 7 \text{ m}^{-1}$ is negligible, while the underestimation in mean can be compensated by the mean adjustment term. Figure 8 and 9 also show the SD and mean of footing displacement under single exponential autocorrelation. Compared to squared exponential function, the SD of footing displacement is larger when $\theta < 0.5B$.

To investigate whether VRF can be applied to cases when the variance of the soil property is large, the analysis is repeated with the CV of Young's modulus being 0.4, or standard deviation of 24 MPa, with other problem settings being unchanged. The obtained VRF and MRF curves are plotted in Figures 6 and 7. Unlike statically determinate system, the VRF is higher when the random field variance is larger, which means the variance of footing displacement increases in a faster rate than the soil property variance.

Figures 10 and 11 show the SD and mean of footing displacements obtained from VRF and MRF, with three sets of MCS verification. Compared to small CV case, the discrepancies with the MCS results become more severe,

especially for the mean of footing displacement. A possible explanation is that the principle VRF method is to sum up the contribution of each random field sinusoid independently (Eq. (3)). Meanwhile, for statically indeterminate system, the interaction between the random field sinusoids can be influential, when the Young's modulus has a large variance. However, VRF method has not included this effect.

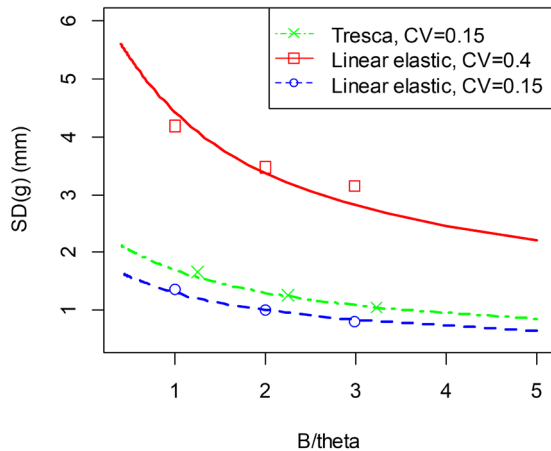


Figure 10: Standard deviation of footing displacement under different autocorrelation distances and soil models.

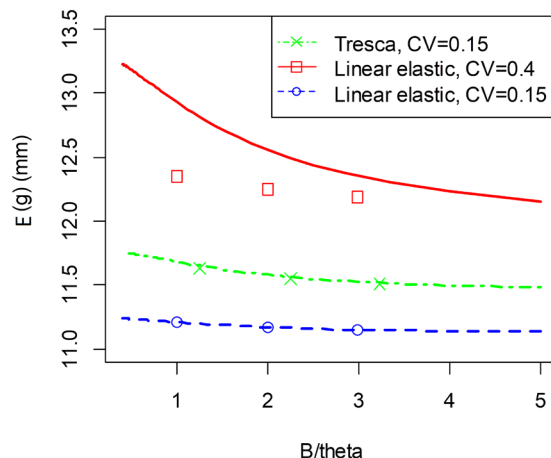


Figure 11: Mean of footing displacement under different autocorrelation distances and soil models.

Apart from linear elastic analysis, footing displacement analysis under Tresca soil is also performed, to examine whether VRF is still applicable when the soil displays non-linear

stress strain behavior. The footing geometry and characteristics of random field of Young's modulus are the same (with CV=0.15), with the only modification being the addition of undrained shear strength s_u , which is perfectly correlated to Young's modulus by $E_u = 300s_u$. The loading is also 514kPa, which corresponds to a deterministic factor of safety of 2, according to the bearing capacity formula $q = (2 + \pi)s_u$. The same ω points and phases are selected, leading to 180 *FLAC* analyses. Again, Figures 6 and 7 show the computed VRF and MRF points with the interpolated curves, and Figures 10 and 11 show the displacement statistics under different θ , with three sets of MCS validation. The MCS statistics match well with the VRF statistics, hence VRF method can be applied to soils with non-linear stress strain behavior. Both VRF and MRF under Tresca soil have larger values than the elastic soil, due to the plastic strains developed. As a result, the mean and SD of footing displacement are both higher than the linear-elastic soil.

4. CONCLUSIONS

This paper outlines the framework of the VRF method, which can analyze the reliability of geotechnical system, when the soil properties exhibit a range of spatial autocorrelation distances and functions. VRF only requires a single set of analysis, while conventional MCS requires separate set of analysis for each spatial autocorrelation setting. In the footing displacement analysis, there is a satisfactory match between the VRF and MCS results, when the soil property has relatively low variance.

Further studies can be pursued to validate and enhance the usefulness of the VRF method. The applicability of VRF should be investigated for strength mobilization problems such as slope stability and bearing capacity. Conceptually, VRF can be applied to 2D and 3D random fields, with the random field being spatially anisotropic, meaning autocorrelation distances are different in each direction. Therefore, VRF has the potential for assessing the system reliability

under spatial anisotropy of soil properties, with minimal computational cost. Meanwhile, when the soil property has a large variance, extensions on the VRF method are necessary, as to incorporate the interaction between the sinusoids that comprise the random field.

5. ACKNOWLEDGEMENTS

The work presented this paper is financially supported by the Research Grants Council of the Hong Kong Special Administrative Region Government (Project No. 15212418).

6. REFERENCES

- Al-Bittar, T. and Soubra, A.-H. (2014). "Probabilistic analysis of strip footings resting on spatially varying soils and subjected to vertical or inclined loads." *Journal of Geotechnical and Geoenvironmental Engineering*, 140(4), 04013043.
- Ching, J., Wu, S.-S., and Phoon, K.K. (2016). "Statistical characterization of random field parameters using frequentist and Bayesian approaches", *Canadian Geotechnical Journal*, 53(2), 285-298.
- Leung, Y.F. and Lo, M.K. (2018). "Probabilistic assessment of pile group response considering superstructure and three-dimensional soil spatial variability", *Computers and Geotechnics*, 103, 193-200.
- Manitaras, T.-I., Papadopoulos, V. and Papadrakakis, M. (2017). "Dynamic variability response functions for stochastic wave propagation in soils", *Soil Dynamics and Earthquake Engineering*, 97, 60-73.
- Papadopoulos, V. and Kokkinos, O. (2012). "Variability response functions for stochastic systems under dynamic excitations", *Probabilistic Engineering Mechanics*, 28, 176-184.
- Phoon, K.K. and Kulhawy, F.H. (1999). "Characterization of geotechnical variability", *Canadian Geotechnical Journal*, 36(4), 612-624.
- Shinozuka, M. (1987). "Structural response variability", *Journal of Engineering Mechanics*, 113(6), 825-842.